

Supplementary Materials for  
**Lanthanide transport in angstrom-scale MoS<sub>2</sub>-based  
two-dimensional channels**

Mingzhan Wang *et al.*

Corresponding author: George C. Schatz, g-schatz@northwestern.edu; Chong Liu, chongliu@uchicago.edu

*Sci. Adv.* **10**, eadh1330 (2024)  
DOI: 10.1126/sciadv.adh1330

**This PDF file includes:**

Figs. S1 to S28  
Table S1 to S3  
Notes S1 to S3

## Lanthanide transport in angstrom-scale MoS<sub>2</sub>-based two-dimensional channels

Mingzhan Wang et al.

### All-atom MD simulations

Computational Method: We performed all-atom Molecular dynamics (MD) simulations to study the cooperative transport of mixed REE (La<sup>3+</sup> / Pr<sup>3+</sup> / Sm<sup>3+</sup> / Gd<sup>3+</sup> / Dy<sup>3+</sup>) cations in the MoS<sub>2</sub>-COOH membranes. Our model (**Fig. 3A**) consists of a bilayer MoS<sub>2</sub> sheet acting as a rigid piston wall to exert external pressure, an ion-filled feed region, a multi-layered MoS<sub>2</sub> membrane serving as an ion channel, and a pure water permeate region. The multi-layered MoS<sub>2</sub> membrane can be visualized as extracting two layers of MoS<sub>2</sub> from bulk crystals (2H-MoS<sub>2</sub>) and being modified with corresponding acetate functional groups, while leaving a 12.5 Å interlayer spacing (Mo-Mo distance) that is consistent with the experiment. We built a rectangular box with dimensions 170 Å × 57.2 Å × 54.0 Å, we chose the OPC3 water model, and visualized the model using Visual Molecular Dynamics (VMD)(44). We used the parameters taken from Heinz for the MoS<sub>2</sub> membrane (45). We applied the general AMBER force field (GAFF)(46) for the -COOH functional groups. We selected the 12-6-4 LJ-type nonbonded model for the monovalent/trivalent ions (47, 48).

Molecular dynamics (MD) simulations were performed using the OpenMM package (49) (**Table S3**). We deprotonated half of the MoS<sub>2</sub>-COOH groups, as the experimental observed pH (pH ~ 4.7) is similar to the pKa of acetic acid (pKa ~ 4.76). We put 12 REE into the membrane to neutralize the negatively charged membranes, where the initial position of REE in the membrane is taken from the equilibrium state after applying a force of 300 kcal/mol/nm (see snapshots in **Fig. S18**). Note that here the ratio of REE inside the membrane is: La<sup>3+</sup>/Pr<sup>3+</sup>/Sm<sup>3+</sup>/Gd<sup>3+</sup>/Dy<sup>3+</sup> = 1:2:4:3:2, which was based on the experimental uptake results (**Fig. S13A**). Note that the ratio in MD

simulations deviates slightly from the experimental ratios because we need to consider the following three factors simultaneously: 1) We have to ensure that the total number of ions is 12 to achieve membrane equilibrium, 2) We need to keep the number of each species as an integer, 3) We want the ratio of rare earth elements within the membrane to form a volcano shape.

There are several noteworthy points we want to point out. Firstly, it is essential to recognize that the simulated mixture employed in this study, encompassing five REE cations, represents a simplified representation in comparison to the experimental setup, which involved a mixture containing thirteen REE cations. This simplification arises from constraints associated with the size scale of our computational simulations. Nonetheless, the trends extracted from our simulations align well with the experimental observations and provide atomistic-level insight into the underlying mechanisms governing REE ion transport. Secondly, due to the lack of parameters in the 12-6-4 model of nitrate anion, we used  $\text{Cl}^-$  in our simulation instead of the nitrate anion used in the experiment. We chose  $\text{Cl}^-$  for two reasons: 1. its diffusion coefficient is similar to that of nitrate anion(50); 2. it is a commonly used anion in MD simulations(51). In addition, calculation of the radial distribution function (RDF) of REE and  $\text{Cl}^-$  in the bulk solution shows that Ln-Cl does not form ion clusters in the simulation (**Fig. S17**).

All the systems were subject to a 10000-step energy minimization followed by a 5 ns NVT ensemble at 300 K using Langevin dynamics to equilibrate the system. The piston wall and membrane are positionally restrained, whereas ions are restrained to pass through the channel by applying a flat-well potential. We then removed the constraints on the ions and performed the non-equilibrium production simulations in the NVT ensemble where external pressures (**Table S3**)

were applied on the rigid piston wall to simulate ions permeating through the MoS<sub>2</sub>-COOH membrane(52). The temperature was kept at 300 K using a Langevin thermostat with a friction coefficient of 1 ps<sup>-1</sup>. The particle mesh Ewald method was employed to calculate electrostatic interactions with a short-range cutoff of 1.0 nm(53). Periodic boundary conditions were employed, and with a simulation time step of 2 fs. To speed up the MD simulations and collect sufficient statistics in the simulations at the ns scale, we employed external pressures higher than the experimentally measured osmotic pressure (~0.5 MPa). Atomic coordinates are saved every 20 ps.

To validate the accuracy of the ion parameters we used in this work, we applied steered molecular dynamics (SMD) simulations to calculate the potential of mean force (PMF) of a single La<sup>3+</sup> or Pr<sup>3+</sup> or Sm<sup>3+</sup> or Gd<sup>3+</sup> or Dy<sup>3+</sup> ion passing through the MoS<sub>2</sub>-COOH membrane. We first construct a 4-layer MoS<sub>2</sub>-COOH membrane with dimensions 55.0 Å × 57.2 Å × 30.0 Å, while leaving interlayer spacings that are consistent with experiment. We then placed the membrane in a rectangular box of size 100.0 Å × 57.2 Å × 30.0 Å and solvated with 2904 OPC3 water molecules. We kept the MoS<sub>2</sub>-COOH functional group half deprotonated in all systems, 12 La<sup>3+</sup> or Pr<sup>3+</sup> or Sm<sup>3+</sup> or Gd<sup>3+</sup> or Dy<sup>3+</sup> cations were added to neutralize the La<sup>3+</sup> or Pr<sup>3+</sup> or Sm<sup>3+</sup> or Gd<sup>3+</sup> or Dy<sup>3+</sup> system, respectively. For each simulation, we added 1 cation and a corresponding number of Cl<sup>-</sup> ions to neutralize the system, where we placed the cation 10 Å outside the membrane (**Fig. S21A**). Following the equilibration procedure mentioned above, we performed an SMD simulation for 40 ns where the position of cation was increased gradually from an initial -10 Å to a final 30 Å. We used harmonic restraints with a force constant 50 kcal/mol/Å<sup>2</sup> to gradually move the cation from outside of the membrane (distance = -10 Å) to the inside of the membrane. We then used the steered MD trajectories as initial coordinates for our umbrella sampling windows. We used the distance as our reaction coordinate, and we divided the trajectories into 40 umbrella windows with

0.1 nm intervals (-10 Å – 30 Å). We then applied a harmonic potential with force constant 20 kcal/mol/Å<sup>2</sup> to constrain each window to the specific distance along the reaction coordinate. Each umbrella window was simulated for 10 ns, where the first 4 ns was discarded as equilibration. We then calculated the potential of mean force using the weighted histogram analysis method (WHAM)(54), as shown in **Fig. S21C**. Our PMF results match well with the decreasing trend of the interlayer spacing in the REE treated MoS<sub>2</sub>-COOH channel (**Figs. 2C-E**).

For the calculations of HFE, we used the same approach as stated in Merz et al. in a previous publication(55) of parameterizing divalent metal ions for OPC3 water models. Our calculated HFE results are shown in **Fig. 3B**, which follows the hydration enthalpy trend in **Figs. 1 D**.

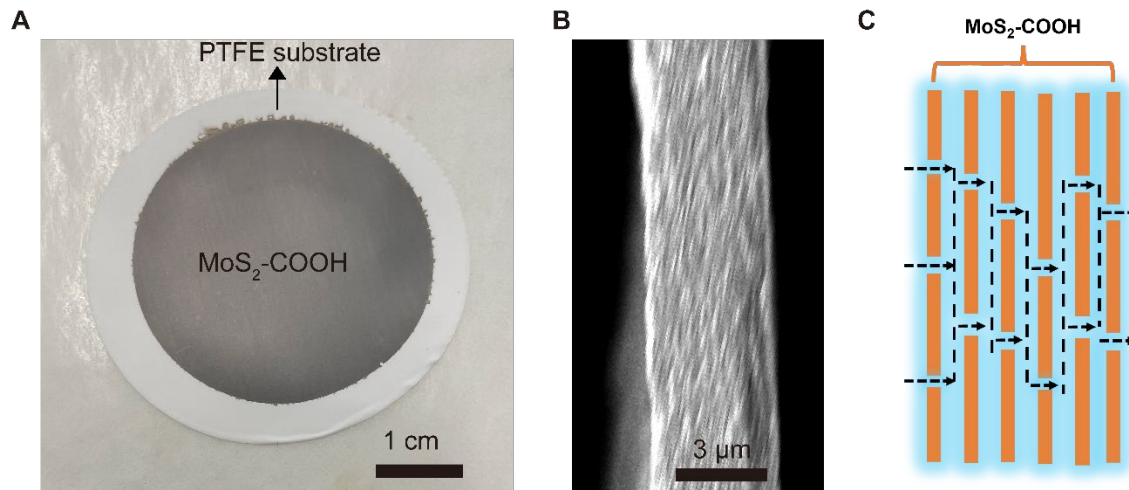


**Fig. S1 MoS<sub>2</sub>-COOH membrane.** (A) Photo of a MoS<sub>2</sub>-COOH membrane filtered onto the porous PTFE substrate (average nominal pore size ~ 200 nm, **Fig. S10** below). (B) Cross-sectional SEM image of the restacked MoS<sub>2</sub>-COOH membranes. (C) Schematic illustration of the ion pathways in the 2D channels of the MoS<sub>2</sub>-COOH membranes.

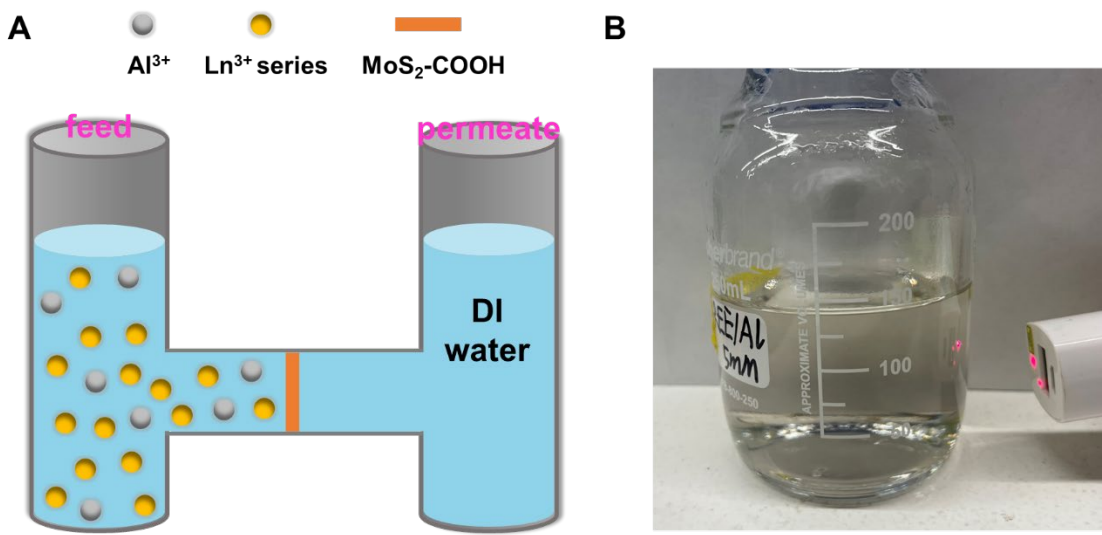


**Fig. S2 Competitive ion separation test across the angstrom-scale 2D channels.** (A) Schematic of the competitive ion separation test. The anion is nitrate, which is omitted for clarity. (B) Photo of the mixture solution containing  $\text{Al}^{3+}/\text{Ln}^{3+}$  ions. The concentration of each cation is  $\sim 5$  mM (pH  $\sim 3.5$ ). No Tyndall effect was observed for the mixture solution.

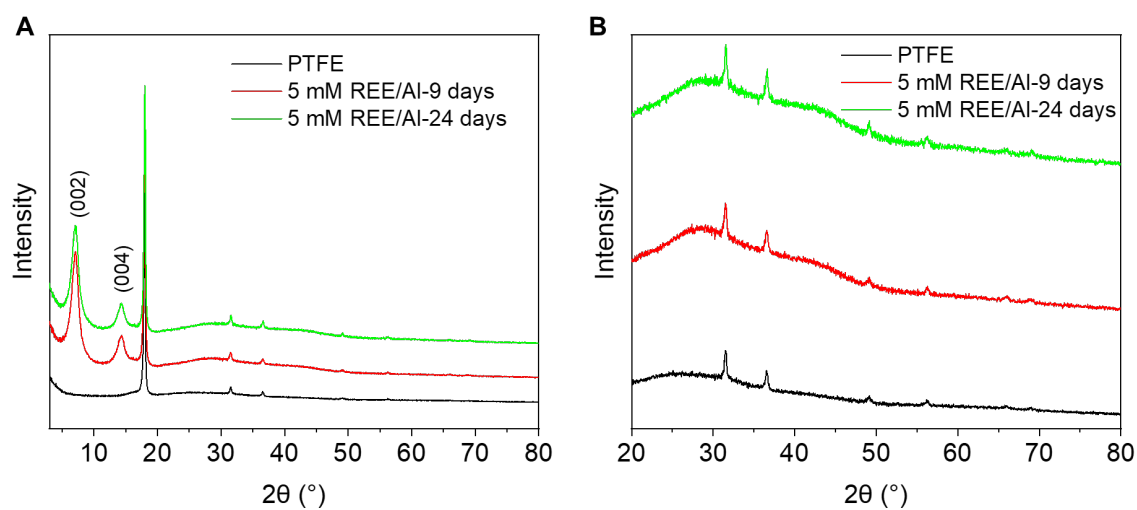


**Fig. S3 Stability of the MoS<sub>2</sub>-COOH membrane in the 5 mM REE/Al mixture solution. (A)** The XRD spectrum of MoS<sub>2</sub>-COOH membrane in 5 mM REE/Al mixture solution for 24 days. **Fig. S3B** is a zoomed-in plot of **Fig. S3A**. No other peak was observed except those belonging to the MoS<sub>2</sub>-COOH membrane and PTFE substrate after 24 days, indicating the MoS<sub>2</sub>-COOH membrane was stable in the REE mixture solution for a relatively long term.

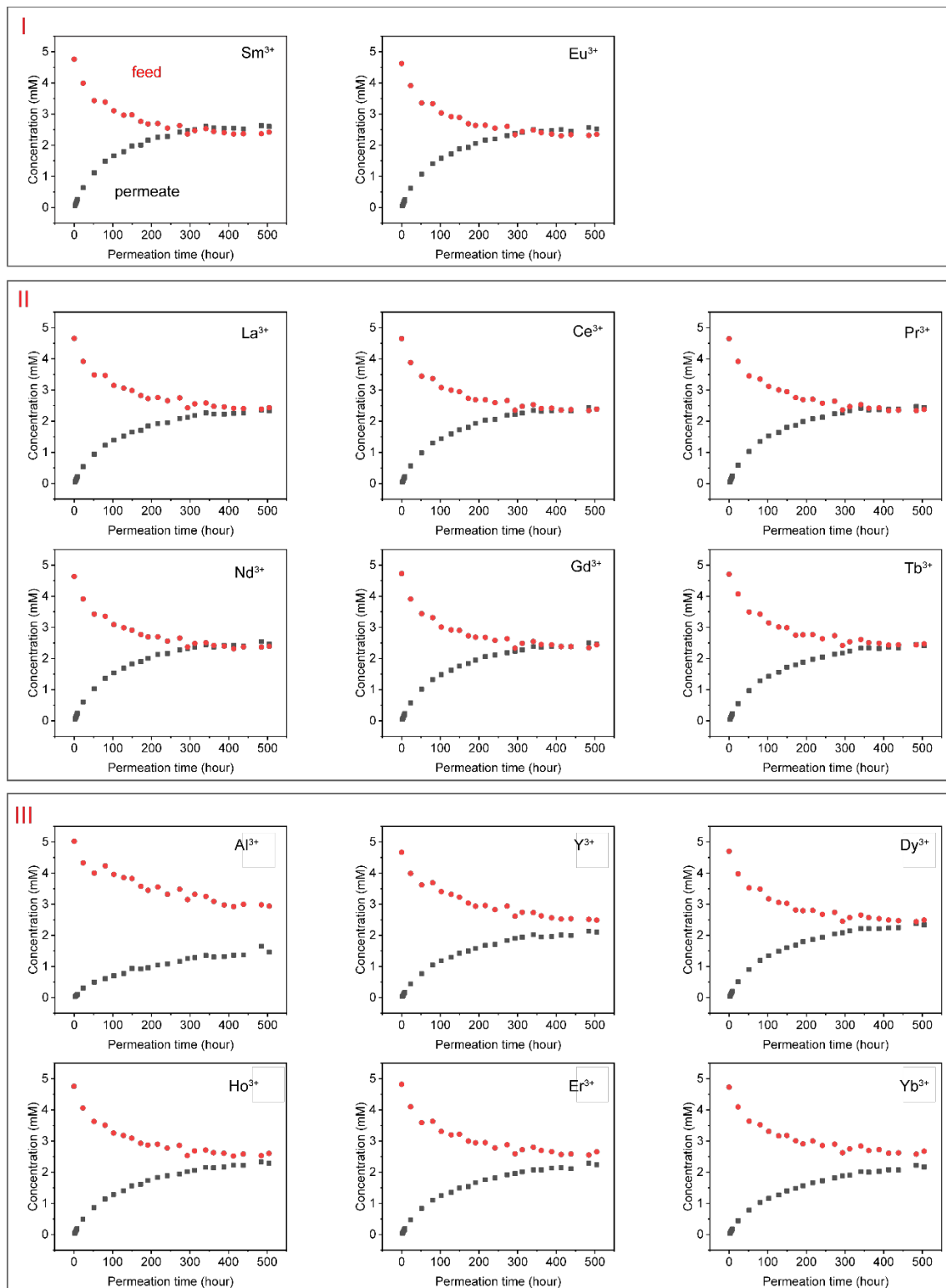


**Fig. S4** The concentration profiles of  $\text{Al}^{3+}/\text{Ln}^{3+}$  cations across the  $\text{MoS}_2\text{-COOH}$  membrane. The concentration profiles are grouped into three types, according to the profile shapes. Cations of type I have a concentration crossover between the feed and the permeate, while type II and type III show concentration equilibria and nonequilibria between the feed and the permeate, respectively.

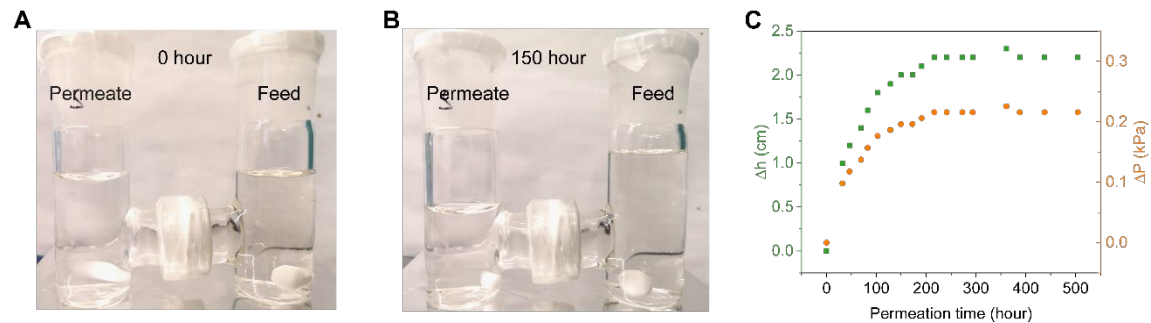


**Fig. S5 Water flow across the MoS<sub>2</sub>-COOH membrane during the permeation test corresponding to Fig. S4. (A) Water level at the beginning of the test. (B) Water level after testing for ~ 150 hour. (C) Evolution of the water level difference  $\Delta h$ , and corresponding hydrostatic pressure difference  $\Delta P$ , between the feed and the permeate during permeation test.  $\Delta P = \rho g \Delta h$ . Since both the solutions are dilute,  $\rho$  takes the value of water density of 1000 kg/m<sup>3</sup>.**

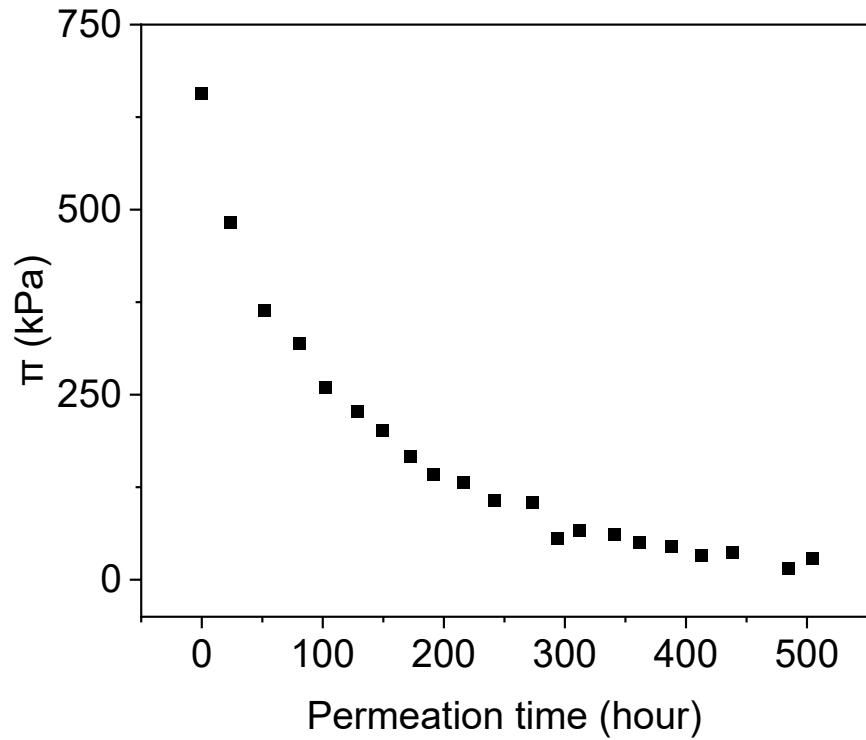


**Fig. S6 Evolution of the osmotic pressure across the MoS<sub>2</sub>-COOH membrane test corresponding to Fig. S4.** The colligative osmotic pressure difference between the feed and the permeate  $\pi = \Delta cRT$ . In the calculations,  $\Delta c$  is the difference of the total concentration of the M<sup>3+</sup> and NO<sub>3</sub><sup>-</sup> between the feed and the permeate, i.e.  $\Delta c = c_{\text{feed}} - c_{\text{permeate}}$ . Since all the salt M(NO<sub>3</sub>)<sub>3</sub> are stoichiometric and the osmotic driven permeation is a charge-neutral process, both  $c_{\text{feed}}$  and  $c_{\text{permeate}}$  is thus four times of the sum of M<sup>3+</sup> measured in the feed or in the permeate, i.e.  $4 \sum c_{\text{M}^{3+}}$ . The activity coefficients of all ions are assumed to be 1, given their low concentrations.

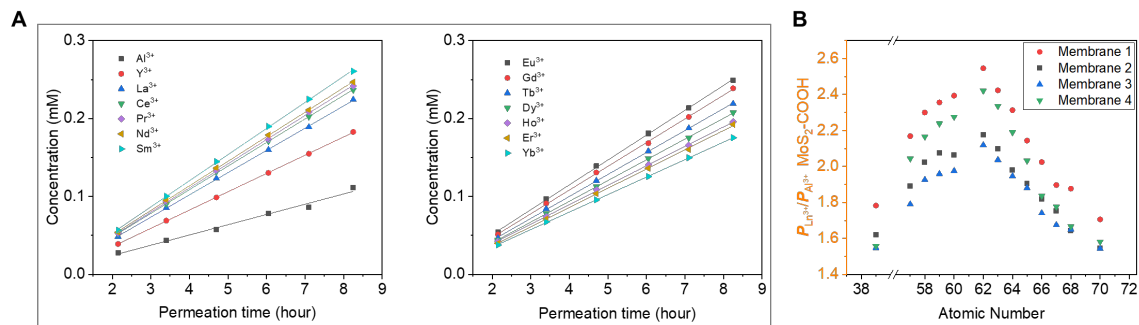


**Fig. S7** Ln<sup>3+</sup> ion transport across the MoS<sub>2</sub>-COOH channels. (A) Representative ion concentration profiles of Ln<sup>3+</sup>/Al<sup>3+</sup> in the permeate side in the early stage, which show linear increase. The permeation rate of the ion  $P_M^{3+}$  is calculated from the slope. (B) Independent transport results across four different MoS<sub>2</sub>-COOH membranes. In the feed, the concentration of each cation is ~ 5 mM in the mixture (pH ~3.5). The permeate is deionized water with natural pH values (DIW, pH ~4-5).

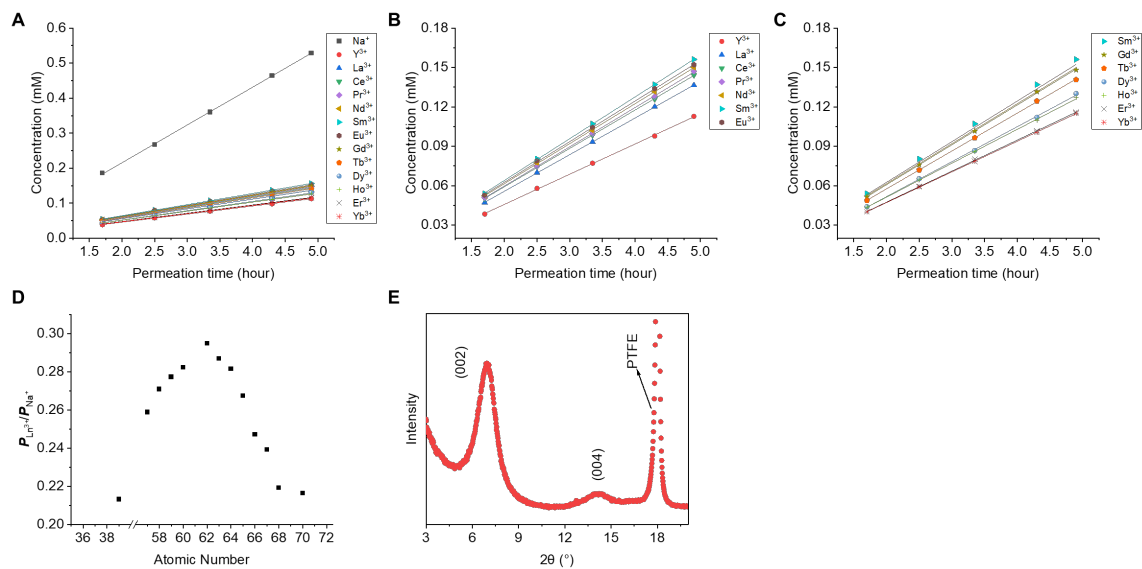


**Fig. S8** Ln<sup>3+</sup>/Na<sup>+</sup> ion transport across the MoS<sub>2</sub>-COOH channels. (A-C) Ion concentration profiles of Ln<sup>3+</sup>/Na<sup>+</sup> in the permeate side in the early stage, which show linear increase. (B) and (C) are the zoomed-in plot of (A). (D) The permeation rate of the ion  $P_{Ln^{3+}}$  across the MoS<sub>2</sub>-COOH membrane referenced to Na<sup>+</sup>. (E) The XRD spectrum of MoS<sub>2</sub>-COOH membrane in 5 mM REE/Na mixture. The effective interlayer spacing for ion transport is 12.6-6.2=6.4 Å.

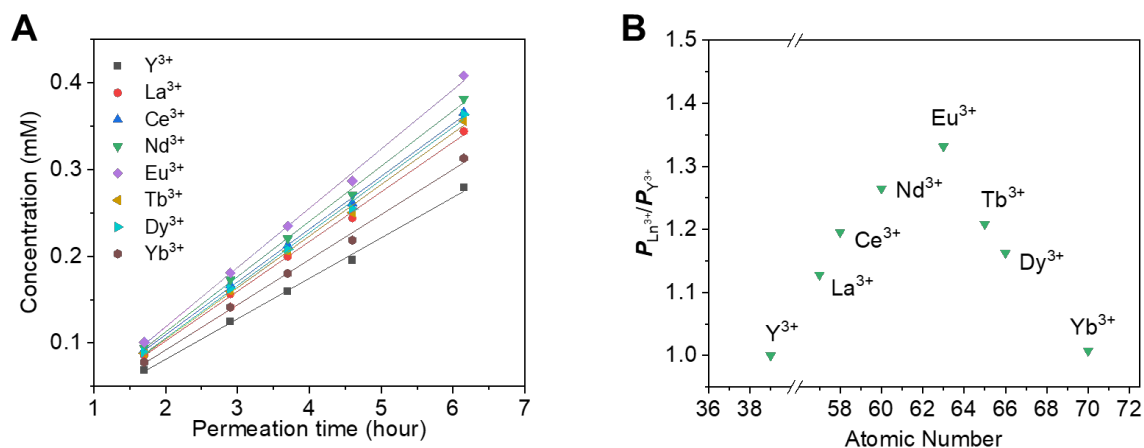


**Fig. S9**  $\text{Ln}^{3+}$  ion transport with combination of  $\text{Y}^{3+}/\text{La}^{3+}/\text{Ce}^{3+}/\text{Nd}^{3+}/\text{Eu}^{3+}/\text{Tb}^{3+}/\text{Dy}^{3+}/\text{Yb}^{3+}$  in the feed ( $\sim 5\text{mM}$ , with natural pH after salts dissolve without further tuning) across the  $\text{MoS}_2\text{-COOH}$  channels. The permeate is deionized water with natural pH values (DIW, pH  $\sim 4\text{-}5$ ). **(A)** Ion concentration profiles for  $\text{Ln}^{3+}$  in the permeate side in the early stage, which show linear increase. **(B)** Permeation rate of  $\text{Ln}^{3+}$  across the  $\text{MoS}_2\text{-COOH}$  membrane.

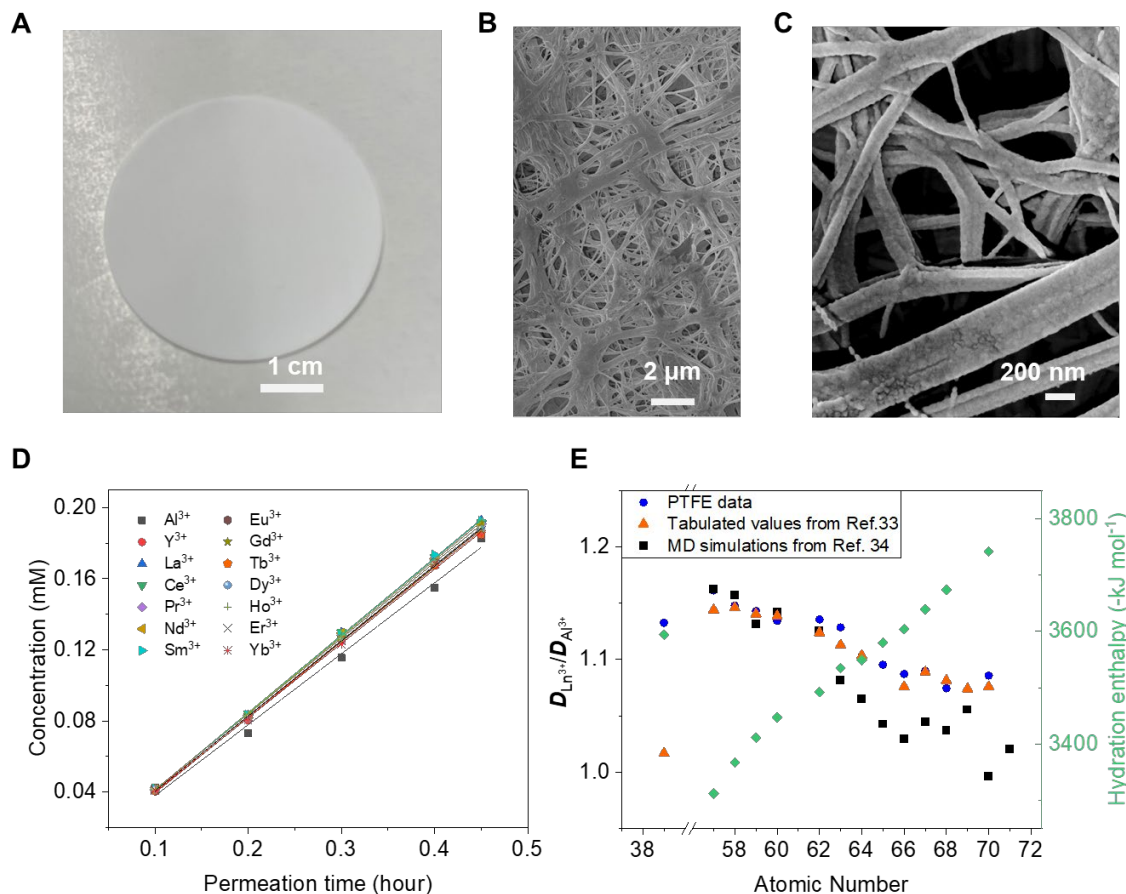


**Fig. S10  $\text{Ln}^{3+}$  ion transport across the porous PTFE membrane.** (A) Photo of the commercial hydrophilic porous PTFE membrane used (nominal pore size:  $0.2 \mu\text{m}$ , purchased from Sigma-Aldrich, Part No. JGWP04700). (B, C) SEM images of the PTFE membrane showing its pores.  $5 \text{ nm}$  Pd/Pt were coated to eliminate the charging effect in imaging. (D) The concentration profiles of all metal cations in the permeate side across the hydrophilic PTFE membrane (pore size  $\sim 200 \text{ nm}$  and thickness  $\sim 65 \mu\text{m}$ ). In the feed, the concentration of each cation is  $\sim 5 \text{ mM}$  in the mixture ( $\text{pH} \sim 3.5$ ). The permeate is deionized water with natural  $\text{pH}$  values (DIW,  $\text{pH} \sim 4-5$ ). (E) Diffusion coefficients of the  $\text{Ln}^{3+}$  cations across the PTFE membrane from measurements and the bulk diffusion coefficients of  $\text{Ln}^{3+}$  from **Refs. 33 and 34** of main text.

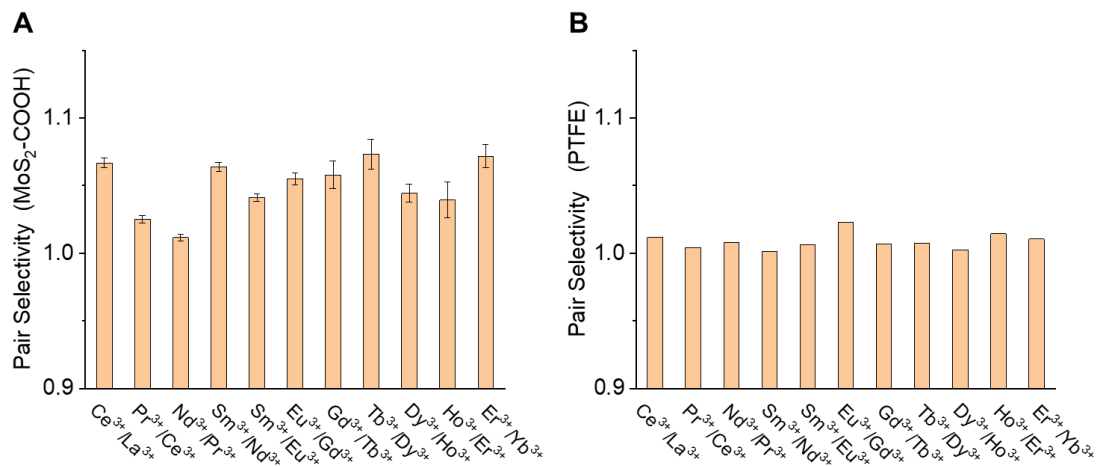


**Fig. S11 Adjacent pair selectivity between Ln<sup>3+</sup> ions in the MoS<sub>2</sub>-COOH membrane (A) and in the PTFE membrane (B).** The data is extracted from the permeability in the transport tests (Figs. 1E and S10E).

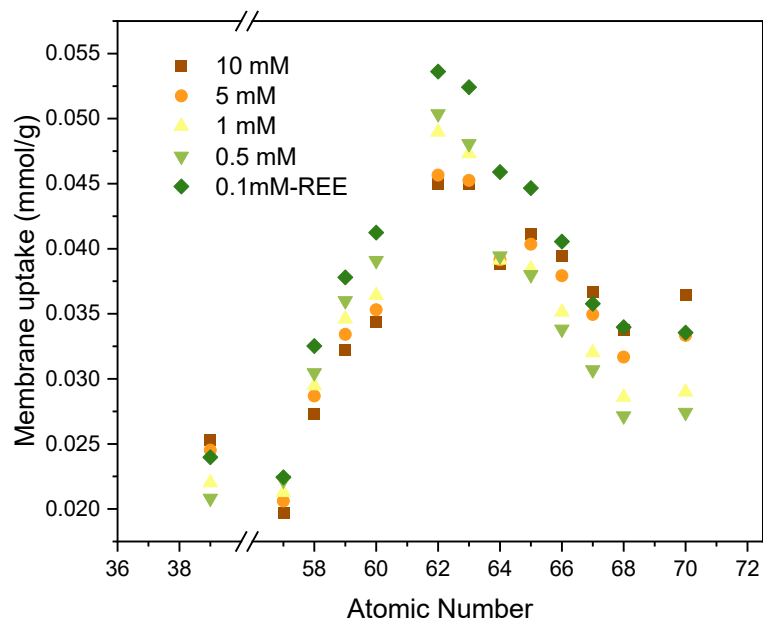


**Fig. S12 Concentration effect of Ln<sup>3+</sup> uptake in the MoS<sub>2</sub>-COOH membrane.**

Uptake condition: mixed Ln<sup>3+</sup> salt solution (2.5 ml), mass of MoS<sub>2</sub>-COOH membrane ~ 0.24 mg, uptake lasted overnight. All the solutions used have their natural pH after salts being dissolved in DI water, i.e. pH ~ 4.70 for 0.1 mM, ~ 4.20 for 0.5mM, ~ 4.02 for 1mM, ~ 3.68 for 5mM, ~ 3.62 for 10mM.

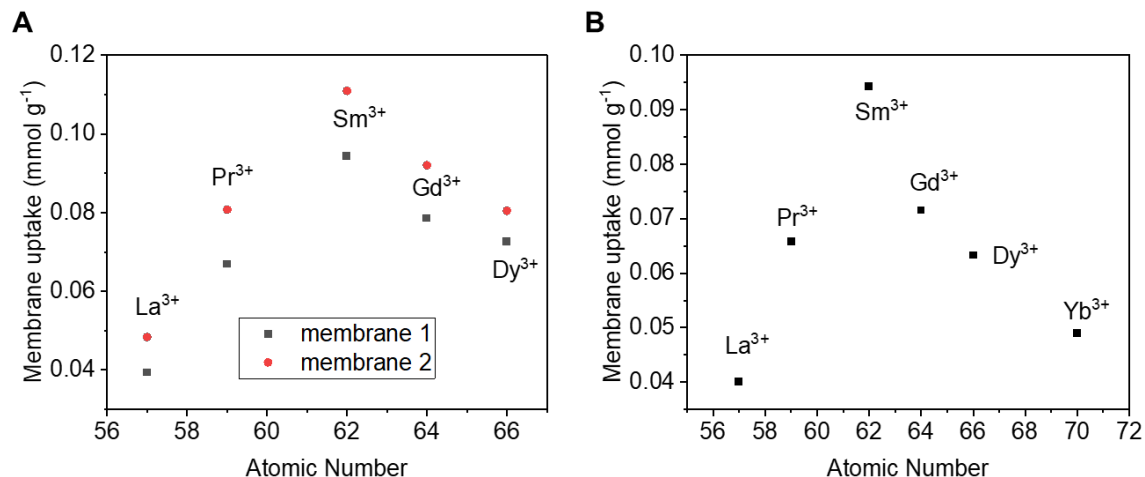


**Fig. S13** The uptake of MoS<sub>2</sub>-COOH membranes to mixed Ln<sup>3+</sup> ions with different combinations. **(A)** La<sup>3+</sup>/Pr<sup>3+</sup>/Sm<sup>3+</sup>/Gd<sup>3+</sup>/Dy<sup>3+</sup> (~5 mM), **(B)** La<sup>3+</sup>/Pr<sup>3+</sup>/Sm<sup>3+</sup>/Gd<sup>3+</sup>/Dy<sup>3+</sup>/Yb<sup>3+</sup> (~5 mM). Both test solutions have natural pH after salts dissolving without further tuning. **Fig. S13A** corresponds to the MD simulations. The uptake ratios of La<sup>3+</sup>/Pr<sup>3+</sup>/Sm<sup>3+</sup>/Gd<sup>3+</sup>/Dy<sup>3+</sup> in membrane 1 and membrane 2 are 1.00:1.70:2.40: 2.00:1.85 and 1.00:1.67:2.30: 1.90:1.67, respectively. **Fig. S13B** corresponds to XAS measurements.

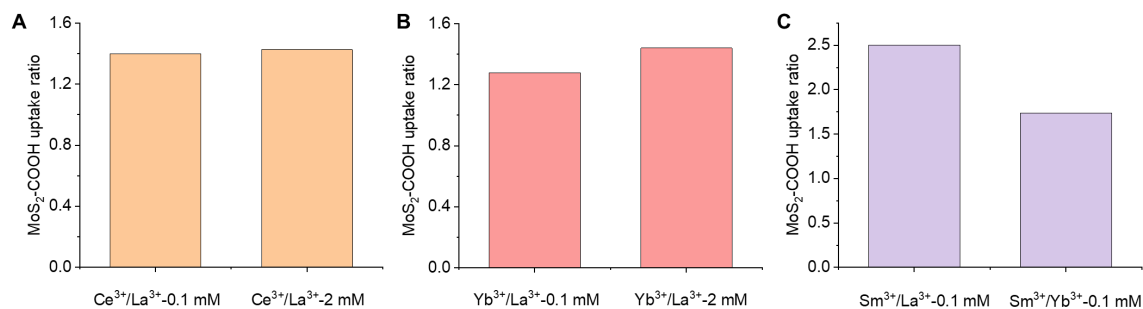


**Fig. S14 Binary uptake results for Ce<sup>3+</sup>/La<sup>3+</sup> (A), Yb<sup>3+</sup>/La<sup>3+</sup> (B) and Sm<sup>3+</sup>/La<sup>3+</sup> and Sm<sup>3+</sup>/Yb<sup>3+</sup> (C) in the MoS<sub>2</sub>-COOH membrane.** To keep the uptake ratio of Ln1/Ln2 above 1 for comparison, Ln1 is the one with a higher uptake amount in all the annotations of the above panels. The concentration indicates the concentration of each lanthanide ion in the binary mixture. All solutions used here have a natural pH after salt dissolving.

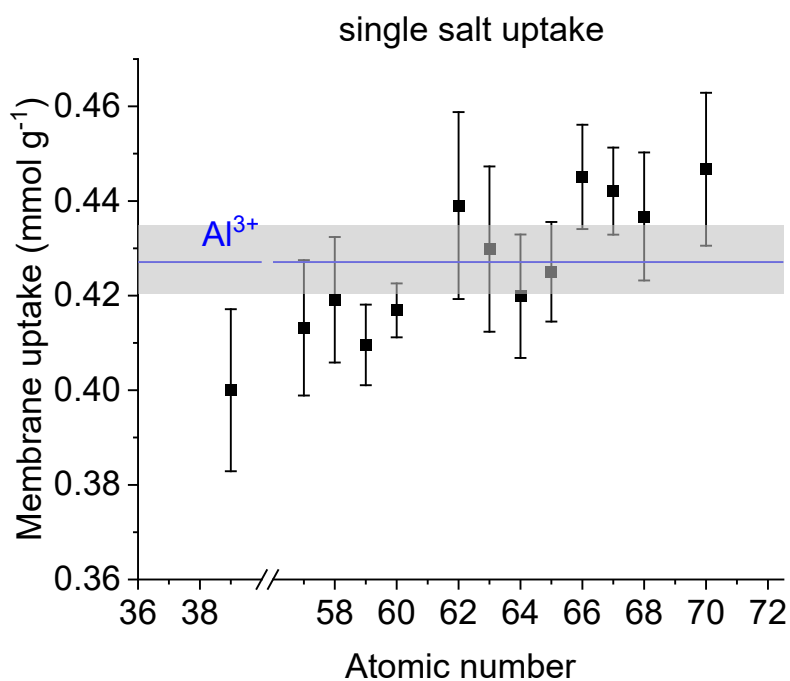


**Fig. S15 Single salt uptake in MoS<sub>2</sub>-COOH membrane.** The shaded area indicates the error bar of Al<sup>3+</sup>. Uptake condition: salt solution (~ 0.1M, 2ml), mass of MoS<sub>2</sub>-COOH membrane ~ 0.3 mg, overnight uptake duration. All single salt solutions have natural pH values after salts dissolving in DI water without further tuning.

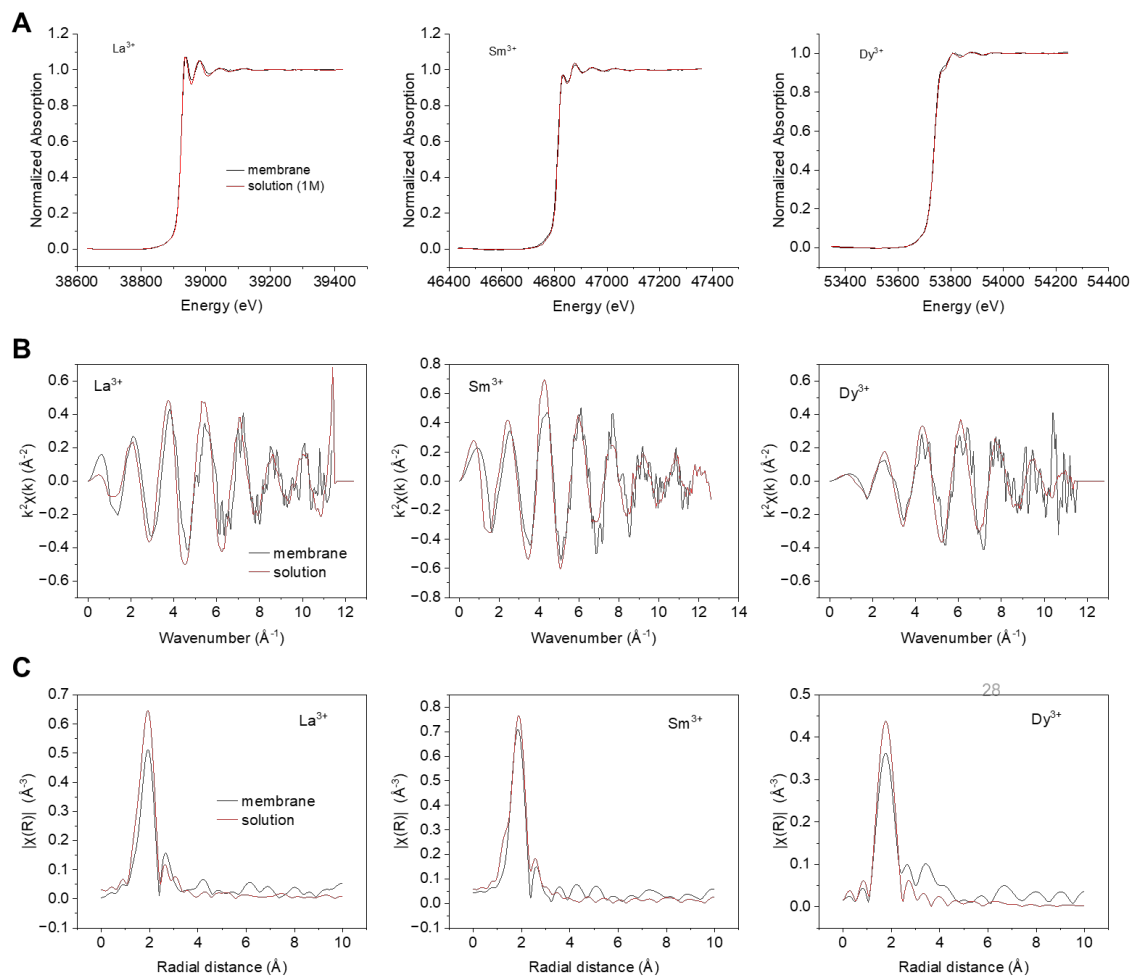


**Fig. S16 X-ray absorption spectroscopy (XAS) measurements.** Panel (A) shows the full XAS spectra of K-edge X-ray absorption of  $\text{La}^{3+}$ ,  $\text{Sm}^{3+}$  and  $\text{Dy}^{3+}$  in their bulk solution and in the  $\text{MoS}_2\text{-COOH}$  membrane. Panel (B) and Panel (C) show the Fourier transformed EXAFS spectra corresponding to Panel (A) in the  $k$ -space and in the  $R$ -space, respectively. Detailed data analyses are shown in Table S1 below. Note that **Fig. S16C** (La) is shown as **Fig. 2F** in the main text.

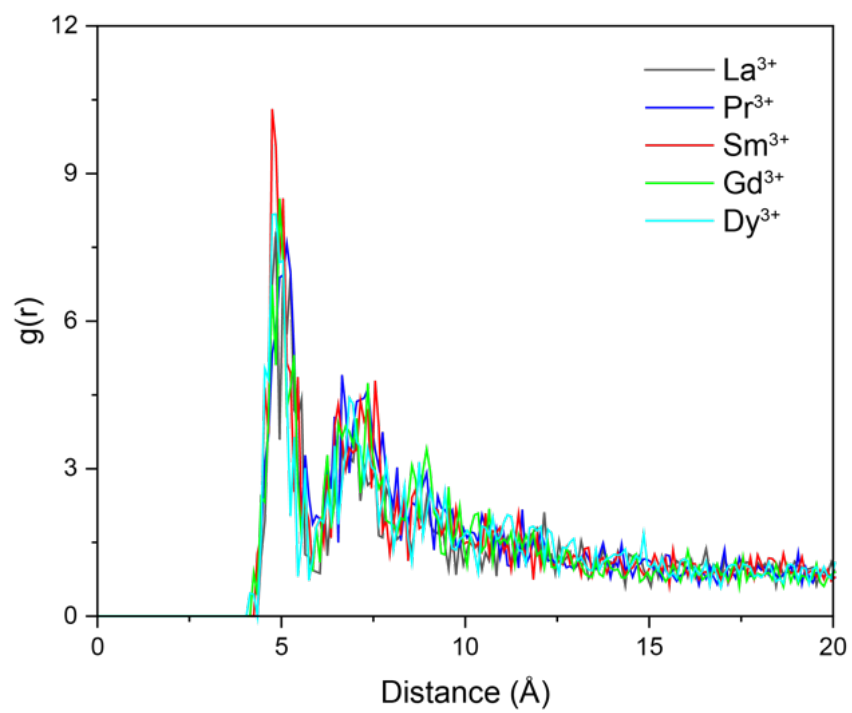


**Fig. S17. Radial distribution function (RDFs) between REE cation and  $\text{Cl}^-$  in the bulk solution.**

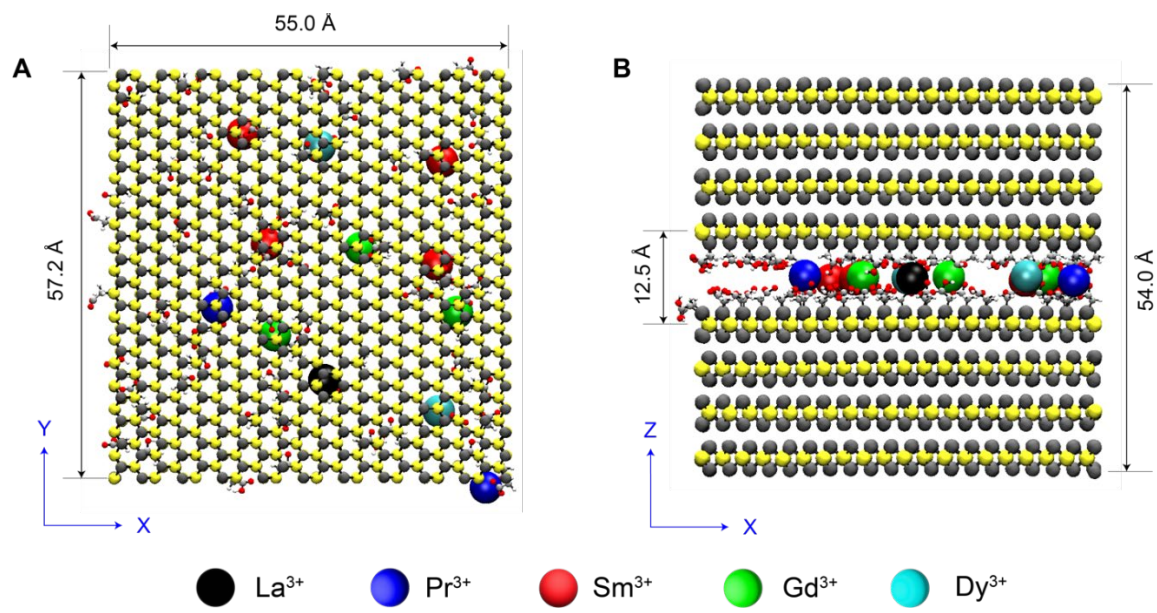


**Fig. S18. Snapshots of the initial position of REE cations in the  $\text{MoS}_2\text{-COOH}$  membrane.** (A) and (B) are the top view and side view, respectively. The ratio of REE cations inside the membrane is:  $\text{La}^{3+}/\text{Pr}^{3+}/\text{Sm}^{3+}/\text{Gd}^{3+}/\text{Dy}^{3+} = 1:2:4:3:2$ , which was obtained based on the experimental uptake results (Fig. S13A).

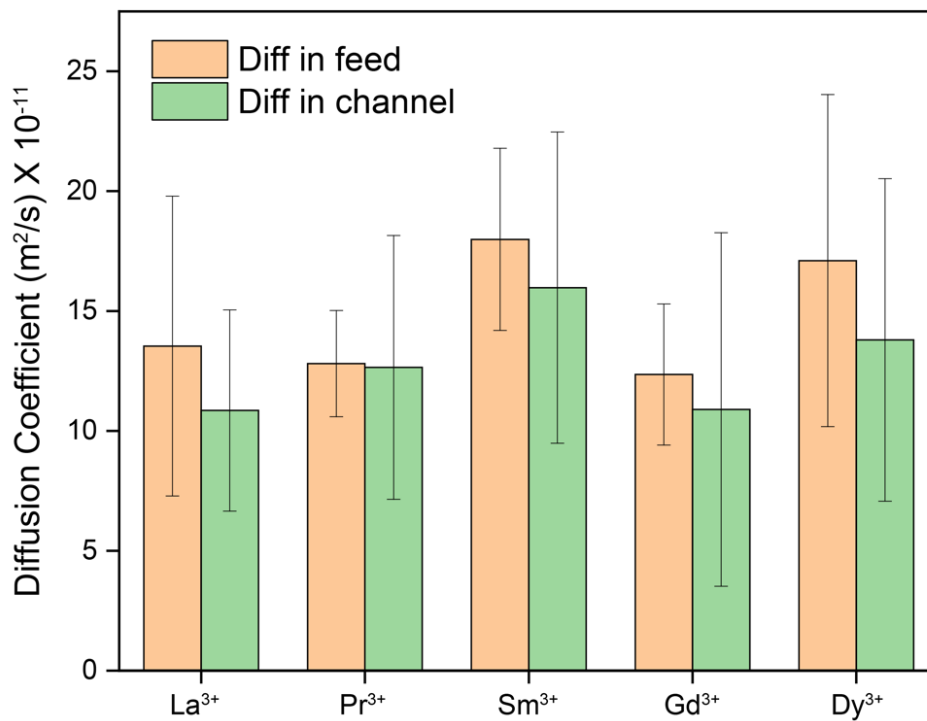


**Figure S19. The diffusion coefficients of REE cations before entering the membrane and inside the membrane.** Here we calculate the diffusion coefficients of each individual ion separately first, and then take average.

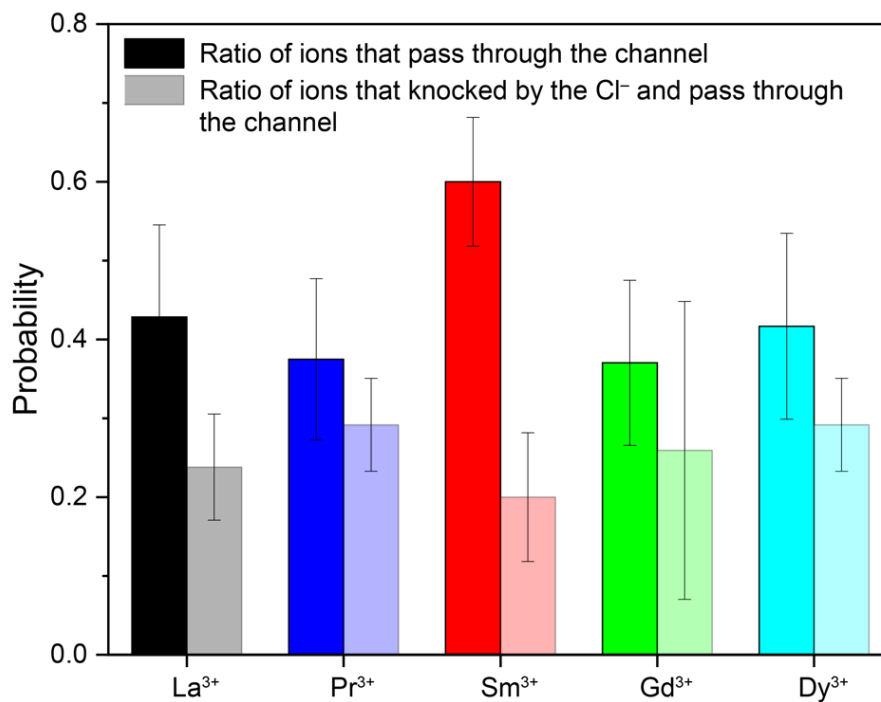


**Fig. S20. The ratio of REE cations that pass through the membrane (solid bar) and the ratio of REE cations that are knocked by Cl<sup>-</sup> and pass through the membrane (transparent bar).** All the data are collected from the averaged values calculated from three independent simulations and the error bars are the standard error of means. Knock was considered to happen if the ions interact at a distance that is 3.5Å or less.

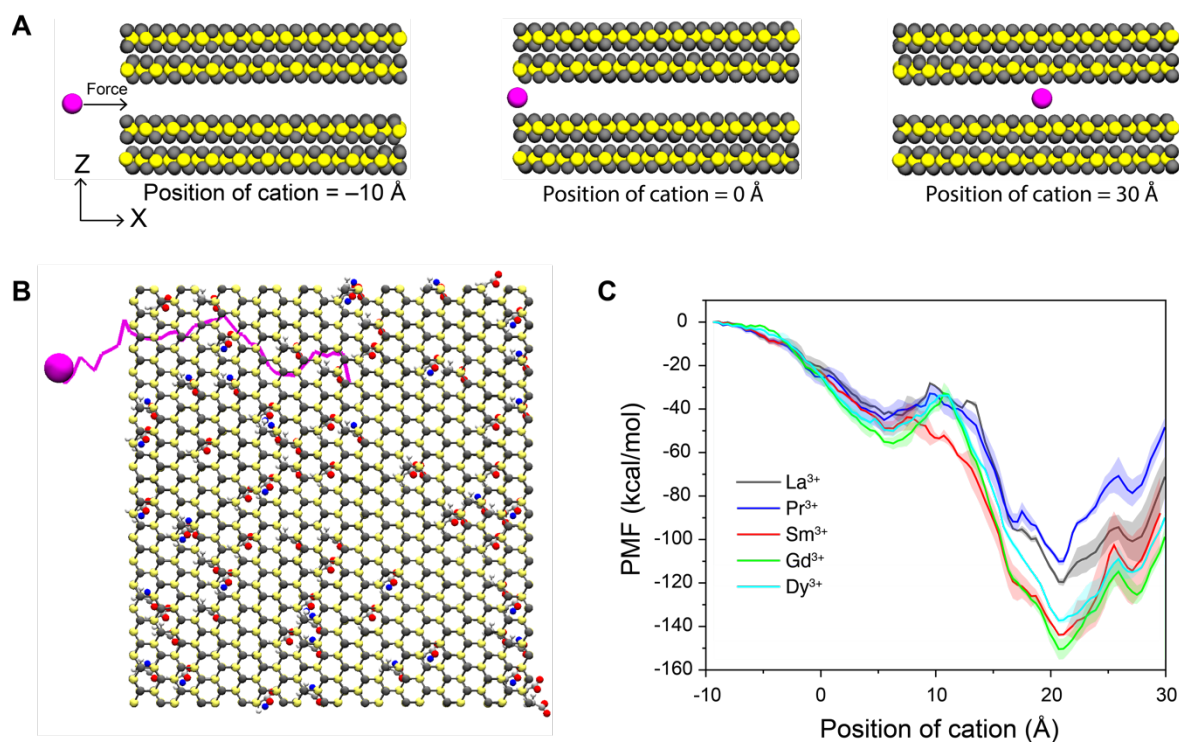


**Fig. S21. PMF calculations.** (A) Snapshots of a REE cation that passing through MoS<sub>2</sub>-COOH membranes. The -COOH group, other ions and water molecules are omitted for clarity. (B) Pathway of REE cation (magenta line) permeating through MoS<sub>2</sub>-COOH channel, in which the -COO<sup>-</sup> group dominant. *Molybdenum, sulfur, carbon, oxygen, alkane hydrogens, and hydroxyl hydrogens are shown in yellow, gray, silver, red, white, and blue beads, respectively.* (C) PMF profiles of ions across the MoS<sub>2</sub>-COOH membrane.

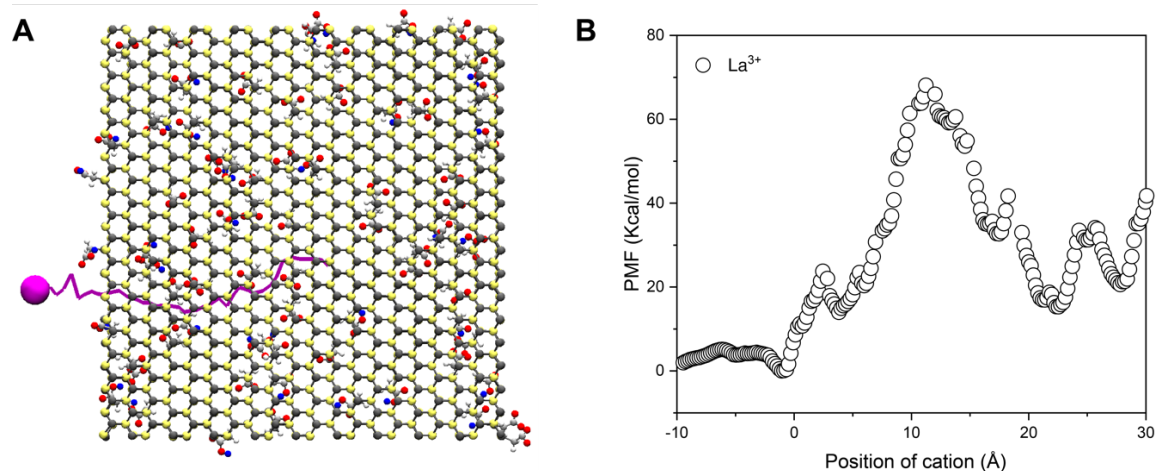


**Fig. S22. PMF calculations incorporating the protonation effect.** (A) Another pathway of  $\text{La}^{3+}$  cation (purple line) permeating through  $\text{MoS}_2\text{-COOH}$  channel, where  $-\text{COOH}$  groups dominate, and the functional group density is higher. *Molybdenum, sulfur, carbon, oxygen, alkane hydrogens, and hydroxyl hydrogens are shown in yellow, gray, silver, red, white, and blue beads, respectively.* (B) The corresponding PMF of  $\text{La}^{3+}$  across the  $\text{MoS}_2\text{-COOH}$  membrane.

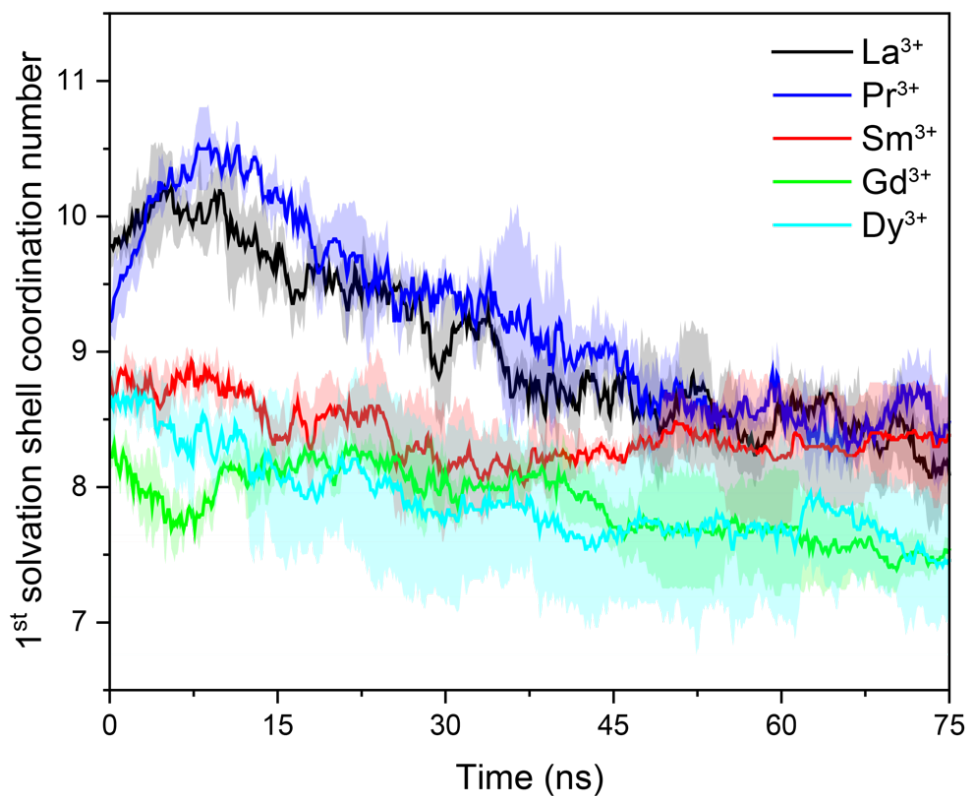


**Fig. S23. The average changes in coordination number in the first solvation shell of REE cations over time.** The time here starts when pressure is initially applied to the rigid piston wall and ends when the rigid piston wall reaches the channel entrance. All the data are collected from the averaged values calculated from three independent simulations and the error bars are the standard error of means.

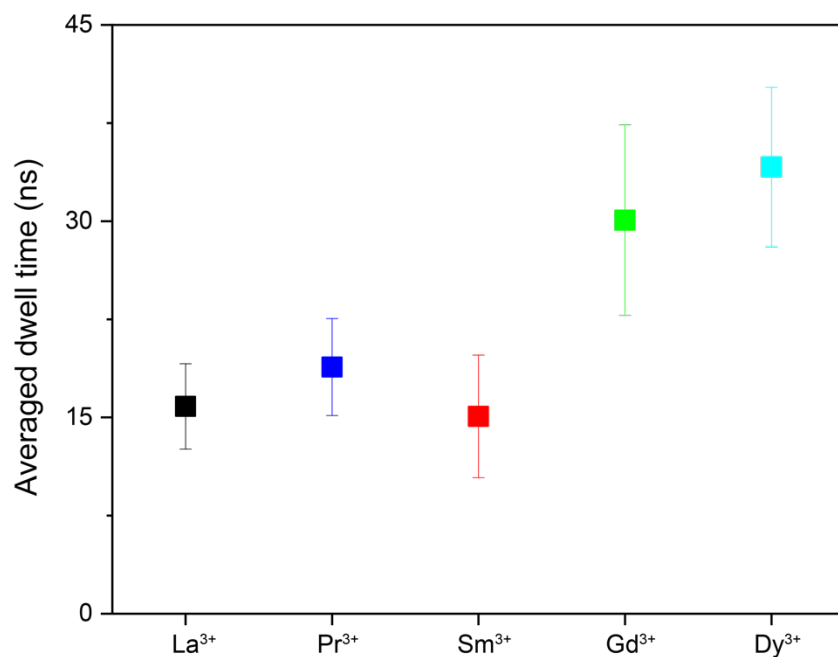


**Fig. S24. Averaged dwell time of REE cations around 3.5 Å of -COOH/-COO<sup>-</sup> group.** All the data are collected from the averaged values calculated from three independent simulations and the error bars are the standard error of means.

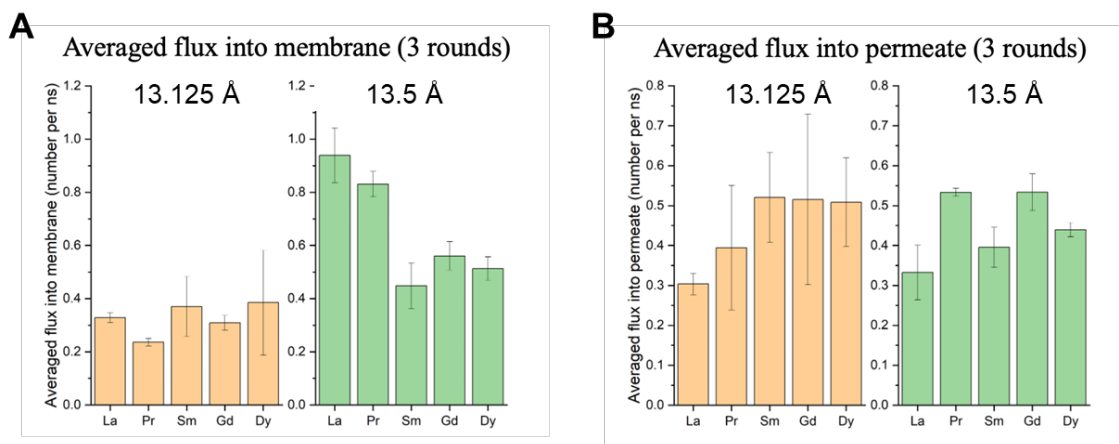


**Fig. S25 MD simulations showing the fluxes of REE cations into the MoS<sub>2</sub>-COOH channel (A), and the fluxes of REE cations into the permeate (B) with interlayer spacings of 13.125 Å (5% increase compared to the one in Fig. 3B, i.e.12.5 Å) and 13.5 Å (8% increase compared to Fig. 3B) in the MoS<sub>2</sub>-COOH channel. All other settings (including the functional group and its density) are kept the same as those in Fig. 3B. Clearly, in the MD simulations of Fig. S25, both the fluxes into the membrane and into the permeate side deviate from the volcano shape presented in Fig. 3B. The deviation confirms the sensitivity of the tradeoff enabling the volcano shape observed in our manuscript.**

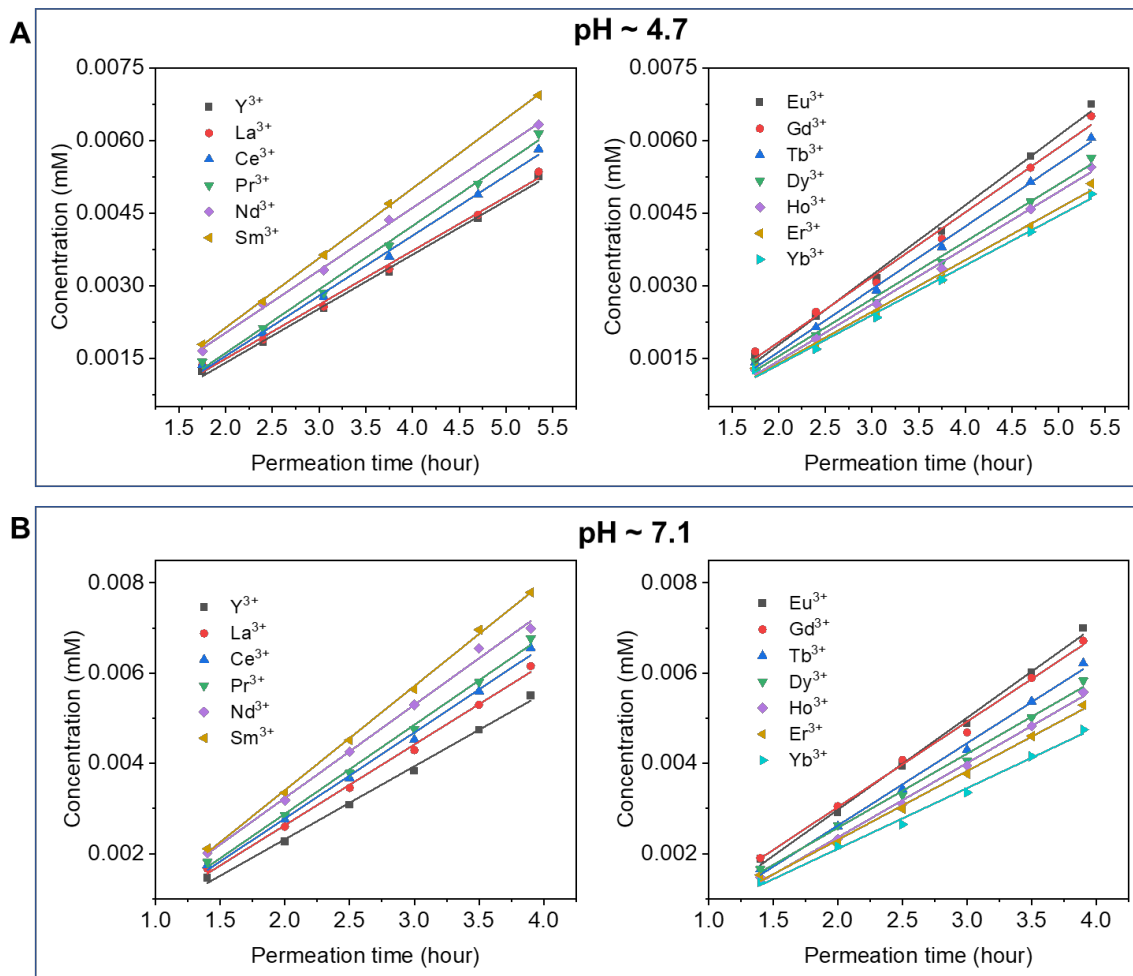


**Fig. S26 pH effect on mixed Ln<sup>3+</sup> transport across the MoS<sub>2</sub>-COOH membrane. (A, B)** Representative ion concentration profiles of Ln<sup>3+</sup> in the permeate side in the early stage at pH ~ 4.7 and ~7.1, respectively. Both tests show linear increase of Ln<sup>3+</sup> in the early stage. The initial feed concentration of both tests was set to be ~ 0.1 mM Ln<sup>3+</sup>. In test (A), pH ~ 4.7 is the natural pH after dissolving mixed Ln(NO<sub>3</sub>)<sub>3</sub> salts (~ 0.1 mM) into DI water, and the initial pH of the permeate side was ~ 5 (DI water). In test (B), we used 0.5M KOH solution to tune the initial pH of both the feed (mixed Ln<sup>3+</sup> solution, ~ 0.1mM) and the permeate (DI water) to be ~7.1.

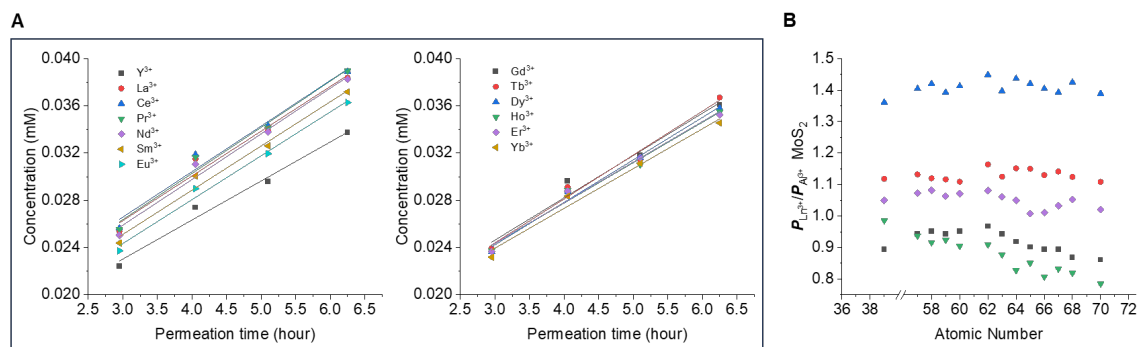


**Fig. S27 Ln<sup>3+</sup> ion transport across the unfunctionalized MoS<sub>2</sub> membrane.** (A) Typical concentration profiles in the permeate side (A) and the permeability (B) of Ln<sup>3+</sup> across the MoS<sub>2</sub> membrane. Each plot in (B) comes from independent transport test of different MoS<sub>2</sub> membranes. In the feed, the concentration of each cation is ~ 5 mM in the mixture (pH ~3.5). The permeate is deionized water with natural pH values (DIW, pH ~4-5). We note that due to the challenge to reversibly control the hydration/dehydration of MoS<sub>2</sub> membrane as we systematically reported in **Ref.31**, the measured ionic fluxes of MoS<sub>2</sub> membranes are usually around or more than one order of magnitude lower than those of MoS<sub>2</sub>-COOH membrane and usually vary a lot among different MoS<sub>2</sub> membranes. This poses a challenge to the accurate measurement of ions, especially for the light Al<sup>3+</sup>. So the fact that some  $P_{Ln^{3+}}/P_{Al^{3+}}$  plots show values smaller than 1, can be attributed to the inaccurate measurement of Al<sup>3+</sup> due to its low concentration. Anyway, the trends are still qualitatively revealing for the transport of lanthanide ions across the unfunctionalized MoS<sub>2</sub> membrane.

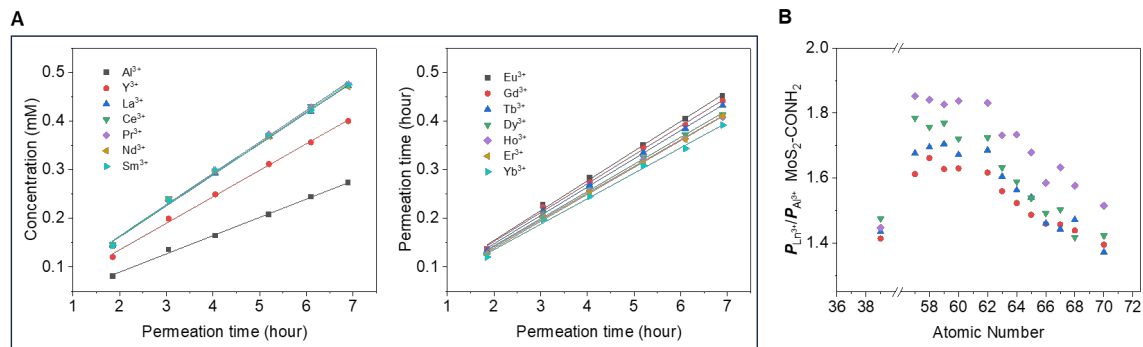


**Fig. S28 Ln<sup>3+</sup> ion transport across the amide-functionalized MoS<sub>2</sub>-CONH<sub>2</sub> membrane. (A)** Typical concentration profiles in the permeate side (A) and the permeability (B) of Ln<sup>3+</sup> across the MoS<sub>2</sub>-CONH<sub>2</sub> membrane. In the feed, the concentration of each cation is ~ 5 mM in the mixture (pH ~3.5). The permeate is deionized water with natural pH values (DIW, pH ~4-5). Each plot in (B) comes from independent transport test of different MoS<sub>2</sub>-CONH<sub>2</sub> membranes. Details of amide functionalization and characterization can be found in our previous work **Ref.31**.

**Table S1. XAS fitting results corresponding to Fig S16.**

	<b>CN</b>	<b>error</b>	<b>R(Å)</b>	<b>error</b>	<b>Dehydration number</b>
La <sup>3+</sup> solution	9.0	0.8	2.56	0.01	
La <sup>3+</sup> membrane	5.7	1.2	2.54	0.11	<b>3.3</b>
Sm <sup>3+</sup> solution	9.0	0.9	2.43	0.01	
Sm <sup>3+</sup> membrane	6.0	0.8	2.40	0.01	<b>3.0</b>
Dy <sup>3+</sup> solution	8	0.5	2.34	0.01	
Dy <sup>3+</sup> membrane	4.7	0.6	2.31	0.03	<b>3.3</b>

CN: coordination number. R: scattering path length.

**Table S2. pH-dependent uptake tests.** Total Ln<sup>3+</sup> uptake in the MoS<sub>2</sub>-COOH membrane and their percentage w.r.t. the -COOH groups in the pH-dependent uptake tests corresponding to **Fig. 4A**.

pH	Total Ln <sup>3+</sup> uptake (mmol g <sup>-1</sup> )	Ln <sup>3+</sup> /-COOH ratio (%)		
		a	b	c
4.7	~ 0.506	35.4	27.3	19.2
6.6	~ 0.764	53.4	41.2	29.0
6.9	~ 1.146	80.2	61.8	43.5
7.1	~ 1.990	139.3	107.3	75.5

**Note 1:** Uptake condition: mixed Ln<sup>3+</sup> salt solution (~ 0.1 mM, 2.5 ml), mass of MoS<sub>2</sub>-COOH membrane ~ 0.24 mg, overnight uptake duration. Same as mentioned above, we used 0.5M KOH solution to tune the pH of mixed Ln<sup>3+</sup> salt solution.

**Note 2:** Column a/b/c corresponds to the results based on the assumption of the functionalization degree of -COOH of 25%/33.3%/50%, respectively. Note we obtained a functionalization degree of ~ 25% from fitting the results of X-ray photoelectron spectroscopy measurements in our previous work **Ref. 31** of the main text, we considered other values here to estimate the effect of functionalization degree. Although 50% functionalization seems impossible from our previous results, we list it here as a reference.

**Note 3: Calculation details using 25% functionalization degree as an example.**

Molecular weight of MoS<sub>2</sub>-COOH:  $M=160+0.25*59=174.75$  g/mol

Molar Concentration of -COOH in MoS<sub>2</sub>-COOH membrane:  $1/174.75*0.25 = 1.431$  mmol/g

Ln<sup>3+</sup>/-COOH ratio at pH=7.1:  $1.990/1.431*100%=139.2\%$

**Table S3. Summary of simulations using all-atom model developed in this study.**

MoS <sub>2</sub> Fun. state	Number of particles	Ion number in Feed	Force (KJ/mol/nm)	Pressure (Mpa)	Ion number in Membrane	Ion number in Permeate	Simulation time (ns)
Half- protonated	49200	6 La <sup>3+</sup> / 6 Pr <sup>3+</sup> / 6 Sm <sup>3+</sup> / 6 Gd <sup>3+</sup> / 6 Dy <sup>3+</sup> / 90 Cl <sup>-</sup>	600	30.24	1 La <sup>3+</sup> / 2 Pr <sup>3+</sup> / 4 Sm <sup>3+</sup> / 3 Gd <sup>3+</sup> / 2 Dy <sup>3+</sup>	0	Run1: 78 ns Run2: 81 ns Run3: 84 ns